

Lattice architecture effect on the cooperativity of spin transition coordination polymers

Daniel Chiruta,^{1,2,3} Catalin-Maricel Jureschi,¹ Jorge Linares,^{2,a)} Yann Garcia,⁴ and Aurelian Rotaru^{1,a)}

¹Faculty of Electrical Engineering and Computer Science & Advanced Materials and Nanotechnology Laboratory (AMNOL), Ștefan cel Mare University, Suceava 720229, Romania

²GEMaC, Université de Versailles Saint-Quentin-en-Yvelines, CNRS-UVSQ (UMR 8635), 78035 Versailles Cedex, France

³LISV, Université de Versailles Saint-Quentin-en-Yvelines, 78140 Velizy, France

⁴Institute of Condensed Matter and Nanosciences, Molecules, Solids and Reactivity (IMCN/MOST), Université Catholique de Louvain, Place L. Pasteur, 1, 1348 Louvain-la-Neuve, Belgium

(Received 3 November 2013; accepted 22 January 2014; published online 7 February 2014)

We have investigated in the framework of the Ising-like model, by means of Monte Carlo Metropolis method with open boundary condition, the architecture effect on the cooperativity of spin transition coordination polymers. We have analyzed the influence of several physical parameters (size, pressure, and edge effects) on different lattice architectures which were in good agreement with reported experimental data. We show that the cooperativity of a spin crossover system, characterized by the same number of molecules and the same short- and long-range interaction parameters, is progressively enhanced when going from a 1D chain to a 1D ladder type lattice and to a 2D square lattice. © 2014 AIP Publishing LLC. [<http://dx.doi.org/10.1063/1.4864035>]

I. INTRODUCTION

Spin crossover (SCO) materials are a fascinating class of switchable molecular solids that continue to attract enormous interest due to their potential technological applications such as sensing devices (temperature, pressure or gas), data storage, displays,^{1–5} molecular switches,^{6,7} etc. The spin state change in SCO molecular materials is communicated by elastic interactions between the switching molecules, thanks to a strong electron-lattice coupling that leads to cooperative phenomena. The experimental progress has been followed closely by theoretical understanding. To describe the complex behavior exhibited by SCO molecular systems, several models such as Ising-like,^{8–12} atom-phonon coupling,^{13–17} or mechano-elastic^{18,19} ones have been used.

In order to use SCO materials to store binary data, the switching between the low-spin (LS) and high-spin (HS) states must be accompanied by a hysteresis loop providing a useful memory effect.²⁰ For this reason, important efforts have been undertaken by coordination chemists, to increase cooperativity of SCO systems. Indeed combining different strategies, such as the insertion between 1D SCO chains of different counter-anions of different size, geometry and charge,^{21,22} hydrogen bonds,²³ π - π interactions,²⁴ etc., allowed to enhanced cooperativity in various systems.

Recently, Bauer *et al.* reported the synthesis and crystal structure of a 1D SCO molecular system featuring a novel ladder structural geometry.²⁵ This report caught our attention given that the authors stressed a cooperativity increase compared to its 1D homologue system. Motivated by these very interesting results, we performed a theoretical study of the lattice architecture effect from 1D to 2D on the cooperativity of SCO systems.

II. THEORY

The SCO has been modeled as a two-level system, described by an Ising-type Hamiltonian. The Hamiltonian has been solved using the Monte Carlo Metropolis algorithm, with open boundary conditions.^{26,27} Here, we compare the thermal behavior of three different systems, i.e., a 1D SCO chain, a 2D ladder type lattice, and a 2D square lattice, which all have been reported experimentally.²⁸

We have focused on the influence of both short- and long-range intermolecular interactions which are known to play an important role on the hysteretic behavior of SCO systems.^{12,29–33}

The Hamiltonian of SCO systems, that includes both short-range (J) and long-range (G) interactions, as proposed in Ref. 12, is given by

$$H = \left(\frac{\Delta}{2} - \frac{k_B T}{2} \ln g \right) \sum_{i=1}^N \hat{\sigma}_i - J \sum_{\langle i,j \rangle} \hat{\sigma}_i \hat{\sigma}_j - G \sum_{i=1}^N \langle \hat{\sigma} \rangle \hat{\sigma}_i, \quad (1)$$

where $\sum_{i=1}^N$ is the sum over all SCO molecules, $\hat{\sigma}$ can take the value $+1$ (when the molecule is in the HS state) or -1 (when the molecule is in the LS state), Δ is the energy gap between the HS and LS states, k_B is the Boltzmann constant, and $g = g_{HS}/g_{LS}$ is the degeneracy ratio.

Short-range interactions are described by the second term of the Hamiltonian and are proportional to the product between the strength parameter J and the sum over all the nearest interacting neighbours. Long-range interactions are described by the third term of the Hamiltonian and are proportional to the average value of the “fictitious magnetization” $\langle \hat{\sigma} \rangle$ and the strength parameter G . Thus, the system’s Hamiltonian (Eq. (1)) can be written in a simplified form as follows:

^{a)}Electronic addresses: jorge.linares@uvsq.fr and rotaru@eed.uvsq.fr

$$H = h \sum_{i=1}^N \hat{\sigma}_i - J \sum_{\langle i,j \rangle} \hat{\sigma}_i \hat{\sigma}_j, \quad (2)$$

where h is the effective field felt by SCO molecules

$$h = \frac{\Delta - k_B T \ln g}{2} - G \langle \hat{\sigma} \rangle. \quad (3)$$

The HS fraction of the system, n_{HS} , is usually given as a function of the “fictitious magnetization” $\langle \hat{\sigma} \rangle$ as $n_{HS} = (\langle \hat{\sigma} \rangle + 1)/2$.

In our simulations, typical thermodynamical values for SCO materials featuring a cooperative spin transition were used: $\Delta S = 50 \text{ J K}^{-1} \text{ mol}^{-1}$ for the entropy change, which corresponds to the following degeneracy value: $\ln g = 6$ and $\Delta H = 10.8 \text{ kJ mol}^{-1}$ for the molar enthalpy change, that corresponds to the following value for the gap energy: $\Delta/k_B = 1300 \text{ K}$.^{34–36} For the thermal dependence of n_{HS} in both heating and cooling modes, we used a temperature step of 0.5 K and 10 different random seeds. We used 100 MC steps for system thermalization and 1000 MC steps to calculate the stable states of the physical system.

III. RESULTS AND DISCUSSION

A. Lattice architecture effect

In order to get insight into the architecture effect on the cooperativity of a SCO system, we have simulated three typical lattice architectures in coordination polymers such as a 1D molecular chain, a 1D ladder type lattice, and a 2D square lattice. Figure 1 shows the thermal dependence of the HS fraction calculated for the three lattice architectures, each composed of 1600 molecules, for two different values of short-range interactions parameter: $J/k_B = 64 \text{ K}$ (left panel) and $J/k_B = 105 \text{ K}$ (right panel), respectively. For $J/k_B = 64 \text{ K}$, the 1D system exhibits a gradual transition as observed for 1D chains with shock absorber spacers;³⁷ a thermal hysteresis is observed for a 1D ladder type lattice and the hysteresis width increases more for a 2D square lattice. A hysteretic behavior is obtained for the 1D system by

increasing the short-range interactions parameter J/k_B from 64 K to 105 K, with the same tendency of the dependence of the hysteresis width on the lattice architecture as discussed in the previous case.

Here, we underline that we can take into account the emergence of the hysteresis loop in a 1D system by introducing into the Hamiltonian of the long-range interactions term, G . For the sake of consistency, we kept G constant for all three investigated architectures. In this way, it can be emphasized the role of inter-chains bridges. This has been already reported in several experimental studies, which showed that by using appropriate intermolecular interactions between chains, it is possible to significantly increase the hysteresis width of a 1D SCO system.^{20,22,23} In our simulations, the contribution of these inter-chain interactions is described by the long-range interactions parameter G .

B. Size effect

Another feature investigated in our work concerns the size effect on the thermal dependence of the HS fraction. The size dependence of the hysteresis width, for the three types of architectures, is presented in Figure 2(a). The dependence of the hysteresis width on the number of molecules is strongly affected by the lattice architecture and follows a behaviour similar to that observed in the framework of other models,^{14,38,39} i.e., the hysteresis width increases with the number of molecules until reaching a critical value where saturation is observed and the size of the system does not affect anymore the hysteresis loop width. Moreover, the saturation width of the hysteresis loop varies from one lattice architecture to another. The critical value of the number of molecules in order to keep the hysteretic properties of the SCO system strongly increases when going from a 2D square lattice to a 1D ladder type lattice and to a 1D molecular chain. These results underline an important aspect regarding the type of SCO system we should use in various applications: as recording media, where a large hysteresis is needed or as sensing devices, where the SCO should present a very smooth gradual transition from one state to the other one as linearly as possible.³

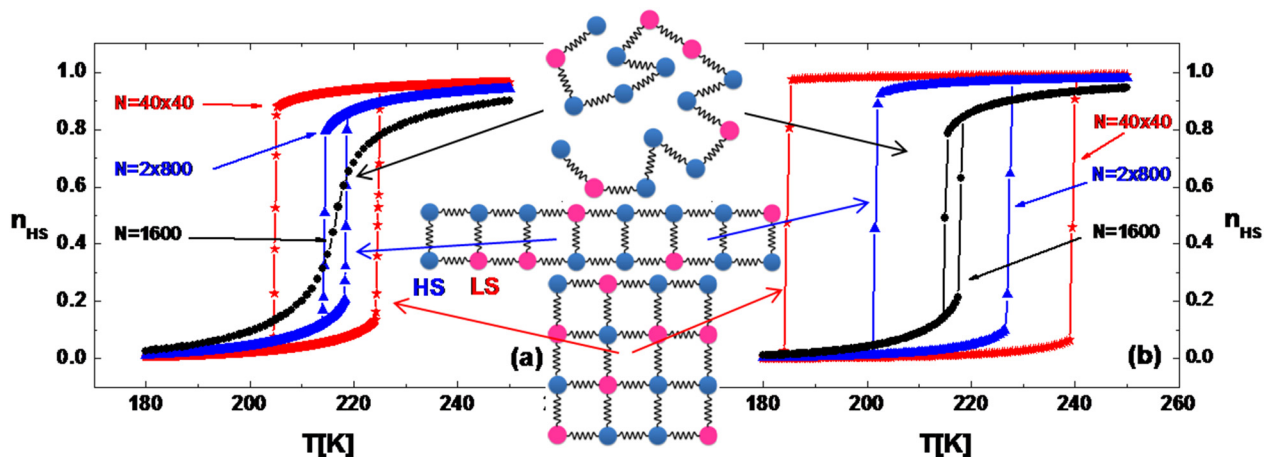


FIG. 1. Simulated thermal hysteresis loops of a square lattice [40×40 molecules] (stars), a 1D ladder type lattice [2×800 molecules] (triangle), and a 1D molecular chain [1600 molecules] (circle) for different values of the short-range interactions parameter: (a) $J/k_B = 64 \text{ K}$ and (b) $J/k_B = 105 \text{ K}$. The values of the parameters used in calculations are $\Delta/k_B = 1300 \text{ K}$, $\ln(g) = 6$, and $G/k_B = 105 \text{ K}$.

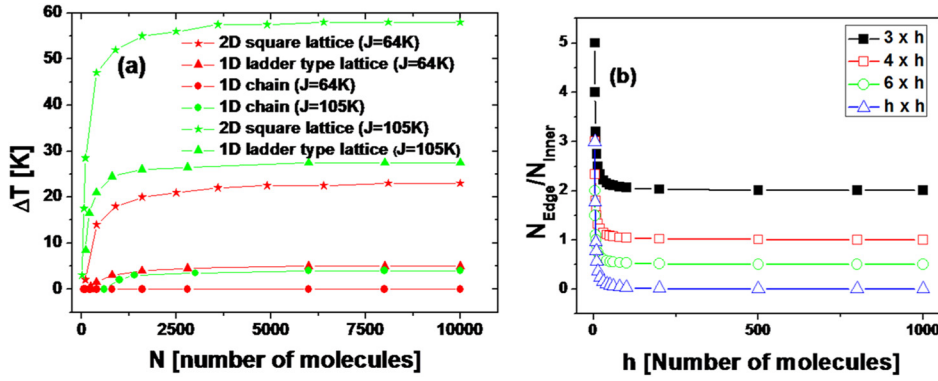


FIG. 2. (a) Variation of hysteresis loop width ΔT vs. number of molecules (N) calculated for the three different types of architectures. The values of the parameters used in the calculations are $\Delta/k_B = 1300$ K, $\ln(g) = 6$, and $G/k_B = 105$ K and (b) variation of edge/inner molecules ratio as a function of system height h , for different lattice architectures.

These differences in the size effect between the different architectures clearly appear from the Edge/Inner molecules ratio and the coordination defects at the system surface, i.e., from the missing bonds due to the creation of the surface. The Edge/Inner molecules ratio for a 2D system can be expressed as follows:

$$\frac{N_{Edge}}{N_{Inner}} = \frac{2(h + w - 2)}{N - 2(h + w - 2)} \quad (\text{for } h \geq w > 2), \quad (4)$$

where h is the height, w is the width of the 2D system, and $N = h \times w$ is the number of molecules.

As we can observe in Figure 2(b), the N_{Edge}/N_{Inner} ratio strongly depends on the considered lattice architecture. By decreasing the width of the system (and keeping the same height), the amount of edge molecules becomes higher than the inner molecules and the effect of the coordination defects on the SCO system cooperativity will be more significant, leading to a decrease of the thermal hysteresis loop width.

C. Influence of short-range and long-range interactions on the hysteresis loop

As previously mentioned, both short- and long-range interactions play an important role on the hysteretic properties of a SCO system.

The critical values of J and G above which the SCO system exhibits a hysteretic behavior are given by Eqs. (5) and (6)^{31,32,40}

$$G_c/k_B = T_0 e^{-q(J/k_B T_0)}, \quad (5)$$

$$J_c/k_B = \frac{T_0}{q} \ln(T_0 k_B / G), \quad (6)$$

where q is the number of neighbours.

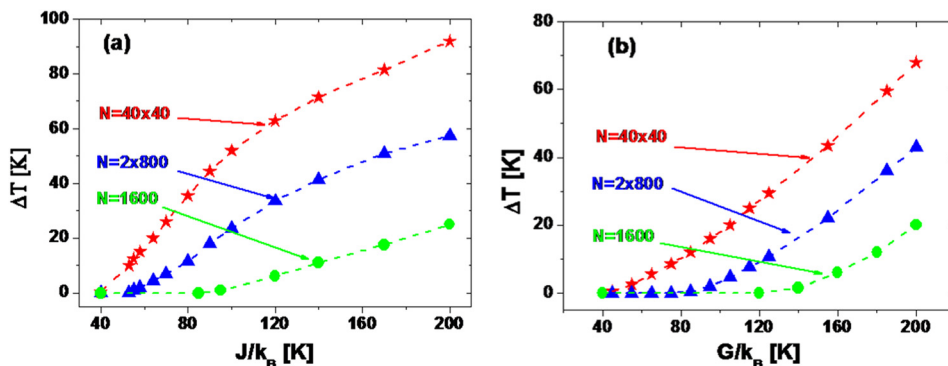


FIG. 3. Evolution of the hysteresis loop width ΔT vs. (a) short-range interactions strength and (b) long-range interactions strength for three different types of architectures: 1D chain (circle), 1D ladder type lattice (triangle), and 2D square lattice (stars). The parameters values are $\Delta/k_B = 1300$ K, $\ln(g) = 6$, and long-range interaction $G/k_B = 105$ K. The parameters values are $\Delta/k_B = 1300$ K, $\ln(g) = 6$, and short-range interaction $J/k_B = 64$ K.

The evolution of the hysteresis width with the short- and long-range interactions, recorded for the three types of lattice architectures, is reported in Figure 3. As it can be observed, the hysteresis width increases with the increase of short- and long-range interactions. However, this dependence is, in addition, strongly affected by the lattice architecture; the 2D square lattice and 1D ladder type lattice are more sensitive to inter-molecular interactions. This difference appears in fact from the different number of neighbors, q , around a SCO molecule in the various lattice architectures: $q = 4$ for the square lattice (or 3 for the edge molecules), $q = 3$ for the ladder type lattice and 2 for the 1D molecular chain.

For very small size, the 1D ladder type and 2D square lattices have a similar hysteretic behavior due to the higher number of molecules on the edge of the lattice comparing to the molecules situated in the inner of the lattice.

1. Analysis of the p - T phase diagram

Due to the change of the metal-ligand distance during the spin state transition, SCO materials are sensitive to the application of an external pressure that will affect the ligand field strength around the central transition ion. In the framework of the Ising-like model, the pressure is acting on the gap energy value as follows:⁴¹⁻⁴³

$$\Delta(p, T) = \Delta + p\Delta V, \quad (7)$$

where Δ is the gap energy at ambient pressure, p is the applied pressure, and ΔV is the volume change of the molecule during the spin state transition. Figure 4 shows the p - T phase diagrams recorded for each lattice architecture. As expected, the critical value of the applied pressure above which the system loses its cooperativity is strongly

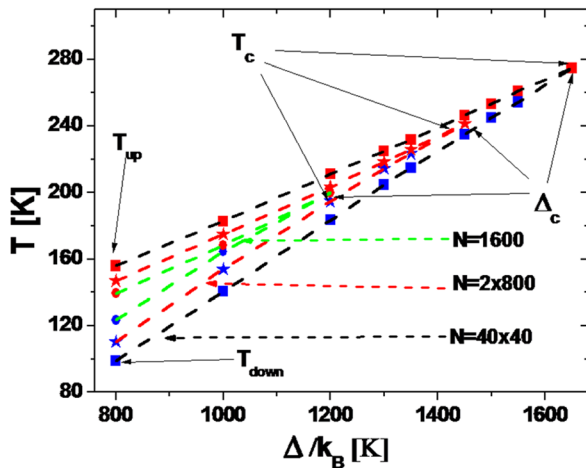


FIG. 4. Phase diagram in p - T coordinates. The values of the parameters used in the calculations are $\ln(g) = 6$, $J/k_B = 64$ K, and $G/k_B = 105$ K.

dependent on the lattice architecture. Since the lowest critical value is obtained on the 1D molecular chain, the highest value of the critical pressure is obtained for the 2D square lattice.

The dependence of the critical temperature T_c and critical pressure Δ_c as a function of short- and long-range parameters, J and G , is displayed in Figures 5 and 6. From these dependencies, one can observe a linear variation of Δ_c and T_c with the interactions parameters. An interesting result is pointed out from the slope of the Δ_c vs. J and T_c vs. J curves recorded for the three lattice architectures.

We can see that the curve recorded for the 1D ladder type lattice is characterized by a slope which is between the 1D and 2D square lattices. For different architectures, the dependences of these critical parameters on the strength of long-range interaction have almost the same slope.

2. Edge effect

When the size of the SCO system is reduced, in some cases, an increase of the residual HS fraction and a lowering of the switching temperatures are observed.⁴⁴ This effect has been theoretically explained by various approaches such as surface energy,⁴⁵ short- and long-range interactions,⁴⁶ or by considering molecules from the surface trapped in the HS state.^{47,48} We have also investigated the edge effect on two different lattice architectures by considering that all the molecules situating on the lattice edge are blocked in the HS state.

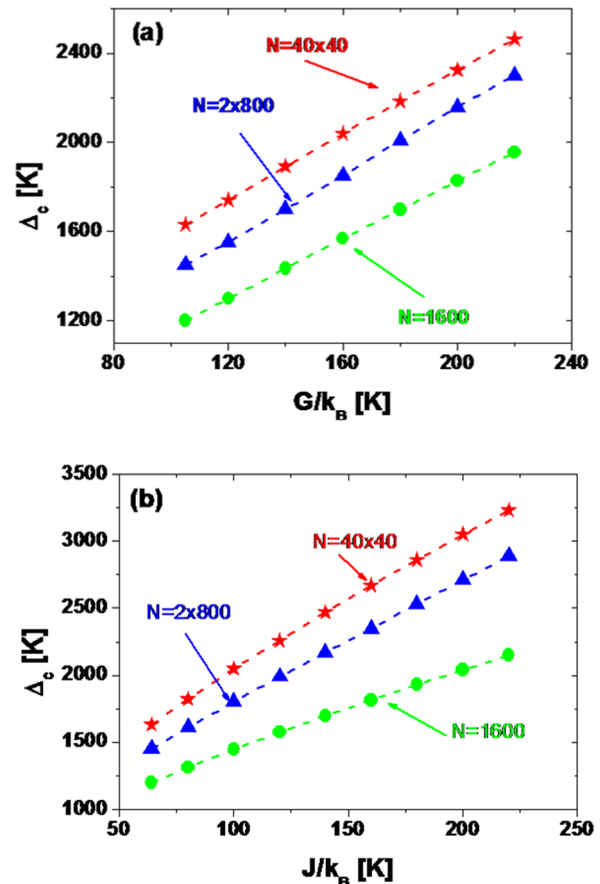


FIG. 5. (a) Evolution of Δ_c vs. long range interactions strength G/k_B . The parameter values are $\ln(g) = 6$ and short-range interaction $J/k_B = 64$ K. (b) Evolution of Δ_c vs. short range interactions strength J/k_B . The parameter values are $\ln(g) = 6$ and long-range interaction $G/k_B = 105$ K.

We have indeed considered a rectangular lattice having (2×800) active molecules of a total number of molecules (4×02) and square lattices having (40×40) active molecules of a total number of molecules (42×42) . The thermal dependence of the HS fraction, taking into account the edge effect (i.e., the molecules from the lattice edge that are blocked in the HS state), is shown in Figure 7. By taking into account these ingredients we succeeded to reproduce the general trend of the experimental results reported in Ref. 43. Thus, by decreasing the dimension of the SCO systems, the switching temperatures shift towards lower temperatures with a decrease of the hysteresis width.

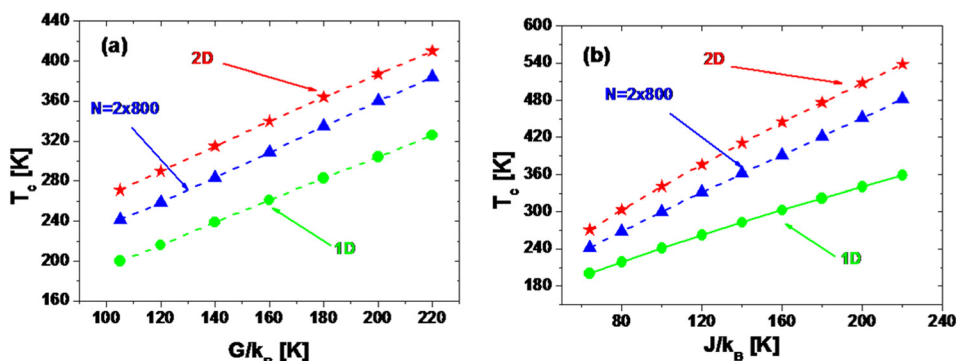


FIG. 6. (a) Evolution of T_c vs. long range interactions strength G/k_B . The parameters values are $\ln(g) = 6$ and short-range interaction $J/k_B = 64$ K. (b) Evolution of T_c vs. short-range interactions strength J/k_B . The parameters values are $\ln(g) = 6$ and long-range interaction $G/k_B = 105$ K.

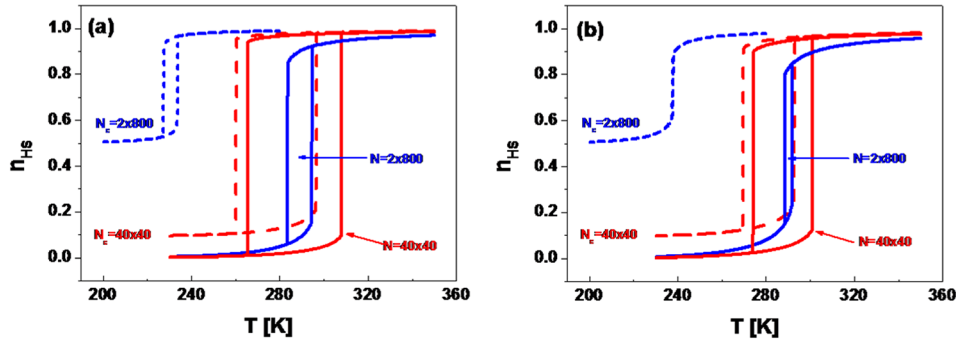


FIG. 7. Comparison of “classic” and edge effect behaviors in the thermal dependences of n_{HS} for a square lattice $[40 \times 40$ active molecules] and rectangular lattice $[2 \times 800$ active molecules] recorded for two different values of short-range interactions: (a) $J/k_B = 124$ K and (b) $J/k_B = 104$ K. The values of the parameters used in calculations are $\Delta/k_B = 1740$ K, $\ln(g) = 6$, and $G/k_B = 105$ K.

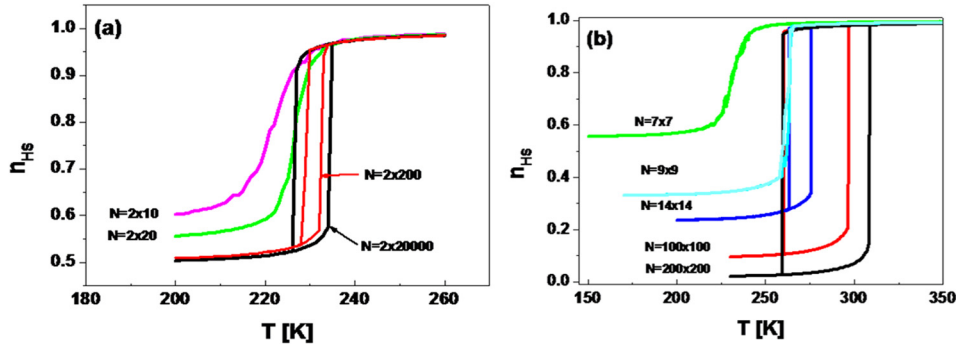


FIG. 8. Thermal dependence of n_{HS} recorded for: (a) rectangular lattice and (b) square lattice for different lattice dimensions. The values of the parameters used in calculations are $\Delta/k_B = 1740$ K, $\ln(g) = 6$, $J/k_B = 124$ K, and $G/k_B = 105$ K.

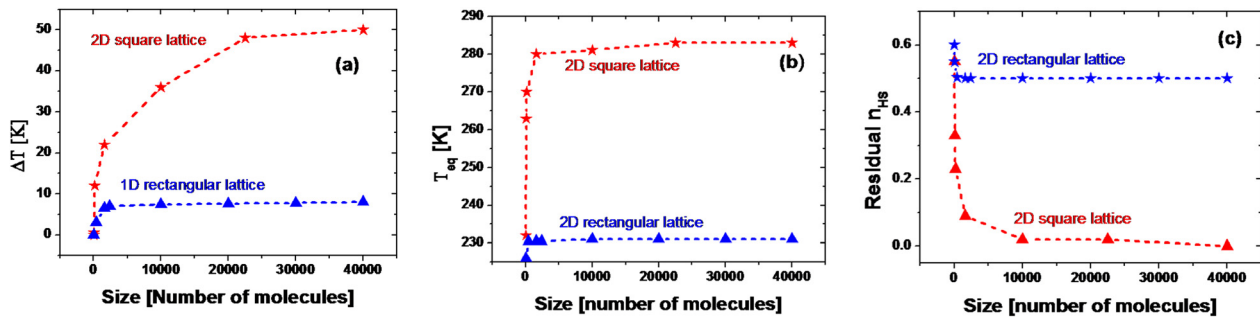


FIG. 9. Size dependence of the hysteresis loop width (ΔT) (a), of equilibrium temperature, T_{eq} (b), and of the residual high spin fraction (c). The parameter values are $\Delta/k_B = 1740$ K, $\ln(g) = 6$, short-range interaction $J/k_B = 124$ K, and long-range interaction $G/k_B = 105$ K.

From the above reported results, it can be observed that the square lattice is less affected by the effect of the low dimensionality than the rectangular lattice (Fig. 8).

Another consequence of the dimension reduction on the thermal behavior is the increase of the residual HS fraction; when the dimension of a SCO system is reduced, the number of the molecules from the edge of the lattice becomes comparable with the number of molecules from the inner of the lattice affecting both the gap energy and the cooperativity of the system.

The variation as a function of the lattice dimension of the equilibrium temperature and of the residual HS fraction is shown in Figures 9(b) and 9(c), respectively. Significant differences between the two lattice architectures (the square and rectangular ($4 \times \frac{Size}{4}$)), if the edge effect is taken into account, are observed in the hysteresis width. Despite the number of molecules are the same in both lattices, the critical temperature above which the hysteresis width saturates is much higher in the 2D square lattice than in the 2D rectangular lattice.

IV. CONCLUSIONS

In this work, we investigated the architecture effect on the hysteretic properties of spin crossover systems from 1D to 2D. Our results are in good agreement with the experiments and give a broader view on the influence of different physical parameters, such as pressure, size, and strength of the long- and short-range interactions. Moreover, we have shown that the cooperativity of a SCO system not only depends on short- and long-range interactions but also strongly on the lattice architecture.

ACKNOWLEDGMENTS

This work was supported by Romanian National Authority for Scientific Research, CNCS—UEFISCDI (PN-II-RU-TE-2011-3-0307), Romanian Academy, WBI-Roumanie, CNCS—UEFISCDI-WIB (Contract No: 587/07.09.2013), Tournesol Hubert Curien, University of Versailles St. Quentin en Yvelines, the Fonds National de la

Recherche Scientifique-FNRS (FRFC 2.4508.08). D.C. thanks to the French Ministry of Foreign Affairs (MAEE) for an Eiffel Scholarship.

- ¹P. Gütllich and H. A. Goodwin, *Spin Crossover in Transition Metal Compounds, Topics in Current Chemistry* (Springer-Verlag, Berlin, 2004), Vol. 233–235.
- ²A. Bousseksou, G. Molnar, L. Salmon, and W. Nicolazzi, *Chem. Soc. Rev.* **40**, 3313–3335 (2011).
- ³J. Linares, E. Codjovi, and Y. Garcia, *Sensors* **12**, 4479–4492 (2012).
- ⁴M. M. Dîrtu, F. Schmit, A. D. Naik, A. Rotaru, J. Marchand-Brynaert, and Y. Garcia, *Int. J. Mol. Sci.* **12**, 5339–5351 (2011).
- ⁵P. Gütllich, A. B. Gaspar, and Y. Garcia, *Beilstein J. Org. Chem.* **9**, 342–391 (2013).
- ⁶A. Rotaru, Il'ya A. Gural'skiy, G. Molnar, L. Salmon, P. Demont, and A. Bousseksou, *Chem. Comm.* **48**, 4163–4165 (2013).
- ⁷A. Rotaru, J. Dugay, R. P. Tan, I. A. Gural'skiy, L. Salmon, P. Demont, J. Carrey, G. Molnar, M. Respaud, and A. Bousseksou, *Adv. Mater.* **25**, 1745–1749 (2013).
- ⁸C. P. Slichter and H. G. Drickamer, *J. Chem. Phys.* **56**, 2142–2160 (1972).
- ⁹A. Bousseksou, J. Nasser, J. Linares, K. Boukheddaden, and F. Varret, *J. Phys. I* **2**, 1381–1403 (1992).
- ¹⁰J. Wajnsflasz and R. Pick, *J. Phys., Colloq.* **32**, C1–91 (1971).
- ¹¹W. Nicolazzi, S. Pillet, and C. Lecomte, *Phys. Rev. B* **78**, 174401 (2008).
- ¹²J. Linares, H. Spiering, and F. Varret, *Eur. Phys. J. B* **10**, 271–275 (1999).
- ¹³J. A. Nasser, K. Boukheddaden, and J. Linares, *Eur. Phys. J. B* **39**, 219–227 (2004).
- ¹⁴A. Rotaru, J. Linares, E. Codjovi, J. Nasser, and A. Stancu, *J. Appl. Phys.* **103**, 07B908 (2008).
- ¹⁵A. Rotaru, J. Linares, S. Mordelet, A. Stancu, and J. Nasser, *J. Appl. Phys.* **106**, 043507 (2009).
- ¹⁶K. Boukheddaden, S. Miyashita, and M. Nishino, *Phys. Rev. B* **75**, 094112 (2007).
- ¹⁷K. Boukheddaden, *Eur. J. Inorg. Chem.* **5–6**, 865–874 (2013).
- ¹⁸C. Enachescu, L. Stoleriu, A. Stancu, and A. Hauser, *Phys. Rev. Lett.* **102**, 257204 (2009).
- ¹⁹M. Nishino, K. Boukheddaden, and S. Miyashita, *Phys. Rev. B* **79**, 012409 (2009).
- ²⁰O. Kahn and C. J. Martinez, *Science* **279**, 44–48 (1998).
- ²¹M. M. Dîrtu, A. Rotaru, D. Gillard, J. Linares, E. Codjovi, B. Tinant, and Y. Garcia, *Inorg. Chem.* **48**, 7838–7852 (2009).
- ²²M. M. Dîrtu, C. Neuhausen, A. D. Naik, A. Rotaru, L. Spinu, and Y. Garcia, *Inorg. Chem.* **49**, 5723–5736 (2010).
- ²³B. Weber, W. Bauer, T. Pfaffeneder, M. M. Dîrtu, A. D. Naik, A. Rotaru, and Y. Garcia, *Eur. J. Inorg. Chem.* **21**, 3193–3206 (2011).
- ²⁴Y. Garcia, J. Moscovici, A. Michalowicz, V. Ksenofontov, G. Levchenko, G. Bravic, D. Chasseau, and P. Gutlich, *Chem. Eur. J.* **8**, 4992–5000 (2002).
- ²⁵W. Bauer, S. Schlamp, and B. Weber, *Chem. Comm.* **48**, 10222–10224 (2012).
- ²⁶J. Linares, J. Nasser, K. Boukheddaden, A. Bousseksou, and F. Varret, *J. Magn. Magn. Mater.* **140–144**, 1507–1508 (1995).
- ²⁷A. W. R. N. Metropolis, M. N. Rosenbluth, A. H. Teller, and E. Teller, *J. Chem. Phys.* **21**, 1087 (1953).
- ²⁸Y. Garcia, N. N. Adarsh, and A. D. Naik, *Chimia* **67**, 411–418 (2013).
- ²⁹A. Rotaru, A. Carmona, F. Combaud, J. Linares, A. Stancu, and J. Nasser, *Polyhedron* **28**, 1684–1687 (2009).
- ³⁰D. Chiruta, J. Linares, P. R. Dahoo, and M. Dimian, *J. Appl. Phys.* **112**, 074906 (2012).
- ³¹D. Chiruta, J. Linares, Y. Garcia, P. R. Dahoo, and M. Dimian, *Eur. J. Inorg. Chem.* **21**, 3601–3608 (2013).
- ³²D. Chiruta, J. Linares, M. Dimian, and Y. Garcia, *Eur. J. Inorg. Chem.* **5–6**, 951–957 (2013).
- ³³S. Klokishner, J. Linares, and F. Varret, *Chem. Phys.* **255**, 317–323 (2000).
- ³⁴M. Sorai, M. Nakano, and Y. Miyazaki, *Chem. Rev.* **106**, 976–1031 (2006).
- ³⁵A. Rotaru, M. M. Dîrtu, C. Enachescu, R. Tanasa, J. Linares, A. Stancu, and Y. Garcia, *Polyhedron* **28**, 2531–2536 (2009).
- ³⁶M. Sorai, Y. Nakazawa, M. Nakano, and Y. Miyazaki, *Chem. Rev.* **113**, PR41–PR122 (2012).
- ³⁷P. J. van Koningsbruggen, M. Grunert, and P. Weinberger, *Monatsh. Chem.* **134**, 183–198 (2003).
- ³⁸A. Rotaru, F. Varret, A. Gindulescu, J. Linares, A. Stancu, J. Létard, T. Forestier, and C. Etrillard, *Eur. Phys. J. B* **84**, 439–449 (2011).
- ³⁹T. Kawamoto and S. Abe, *Chem. Comm.* **31**, 3933–3935 (2005).
- ⁴⁰K. Boukheddaden, J. Linares, H. Spiering, and F. Varret, *Eur. Phys. J. B* **15**, 317–326 (2000).
- ⁴¹A. Rotaru, J. Linares, F. Varret, E. Codjovi, A. Slimani, R. Tanasa, C. Enachescu, A. Stancu, and J. Haasnoot, *Phys. Rev. B* **83**, 224107 (2011).
- ⁴²A. Rotaru, F. Varret, E. Codjovi, K. Boukheddaden, J. Linares, A. Stancu, P. Guionneau, and J. F. Letard, *J. Appl. Phys.* **106**, 053515 (2009).
- ⁴³Y. Konishi, H. Tokoro, M. Nishino, and S. Miyashita, *Phys. Rev. Lett.* **100**, 067206 (2008).
- ⁴⁴F. Volatron, L. Catala, E. Riviere, A. Gloter, O. Stephan, and T. Mallah, *Inorg. Chem.* **47**, 6584–6586 (2008).
- ⁴⁵G. Felix, W. Nicolazzi, L. Salmon, G. Molnar, M. Perrier, G. Maurin, J. Larionova, J. Long, Y. Guari, and A. Bousseksou, *Phys. Rev. Lett.* **110**, 235701 (2013).
- ⁴⁶A. Atitoaie, R. Tanasa, and C. Enachescu, *J. Magn. Magn. Mater.* **324**, 1596–1600 (2012).
- ⁴⁷A. Muraoka, K. Boukheddaden, J. Linares, and F. Varret, *Phys. Rev. B* **84**, 054119 (2011).
- ⁴⁸D. Chiruta, J. Linares, M. Dimian, Y. Alayli, and Y. Garcia, *Eur. J. Inorg. Chem.* **29**, 5086–5093 (2013).